

# WiFi-based Global Localization in Large-Scale Environments Leveraging Structural Priors from osmAG

Xu Ma<sup>1</sup>, Jiajie Zhang<sup>1</sup>, Fuming Xie<sup>1</sup> and Sören Schwertfeger<sup>1</sup>

**Abstract**—Global localization is essential for autonomous robotics, especially in indoor environments where the GPS signal is denied. We propose a novel WiFi-based localization framework that leverages ubiquitous wireless infrastructure and the OpenStreetMap Area Graph (osmAG) for large-scale indoor environments. Our approach integrates signal propagation modeling with osmAG’s geometric and topological priors. In the offline phase, an iterative optimization algorithm localizes WiFi Access Points (APs) by modeling wall attenuation, achieving a mean localization error of 3.79 m (35.3% improvement over trilateration). In the online phase, real-time robot localization uses the augmented osmAG map, yielding a mean error of 3.12 m in fingerprinted areas (8.77% improvement over KNN fingerprinting) and 3.83 m in non-fingerprinted areas (81.05% improvement). Comparison with a fingerprint-based method shows that our approach is much more space efficient and achieves superior localization accuracy, especially for positions where no fingerprint data are available. Validated across a complex 11,025 m<sup>2</sup> multi-floor environment, this framework offers a scalable, cost-effective solution for indoor robotic localization, solving the kidnapped robot problem. The code and dataset are available at <https://github.com/XuMa369/osmag-wifi-localization>.

## I. INTRODUCTION

Global localization, the process of ascertaining a robot’s absolute position within a pre-existing map, underpins the foundation of long-term autonomy in robotic systems. This capability is particularly vital for addressing the robot kidnapping problem in GPS-denied environments, such as indoor spaces, underground facilities, and urban canyons. Although traditional methods relying on Light Detection and Ranging (LiDAR) or vision sensors have demonstrated remarkable success, their deployment is often constrained by high hardware costs, substantial computation demands, and vulnerability to dynamic environmental conditions and they typically fail to solve the kidnapped robot problem. These challenges necessitate the development of alternative localization approaches that are both robust and economically viable.

WiFi-based localization [1]–[3] emerges as a promising alternative, capitalizing on the pervasive wireless infrastructure in modern buildings to deliver a cost-effective and scalable solution, eliminating the need for expensive, specialized hardware. Our work advances this paradigm by proposing a physics-informed localization framework that explicitly models the radio frequency (RF) attenuation caused by physical structures such as walls and doors. The effectiveness of such a physics-informed approach hinges on a map representation that accurately captures the environment’s geometric and

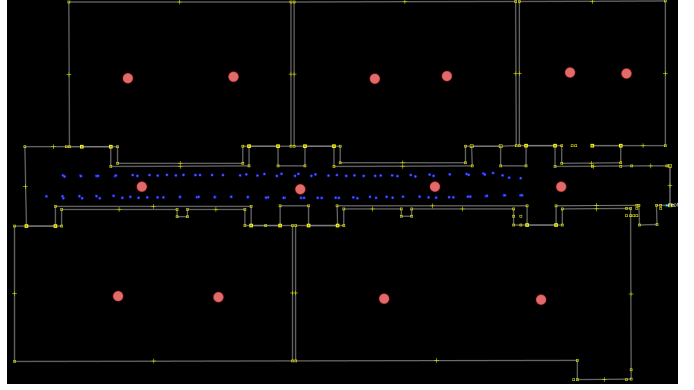


Fig. 1: The osmAG map with domain-specific information is visualized using the JOSM editor [5]. Red points represent WiFi Access Points (APs), blue points indicate robot positions, and yellow polygons delineate the geometric structure of the buildings.

structural features while seamlessly integrating WiFi-specific information. To meet this demand, our system leverages the OpenStreetMap Area Graph (osmAG) representation [4], integrates geometric, topological, and semantic information, making it particularly suitable for indoor robotics applications by enabling precise modeling of complex environments. osmAG, visualized in Figure 1, provides a unified framework that combines three essential components for WiFi-based localization: (1) *geometric representation* through precise coordinate-based node positioning and way-defined spatial boundaries, (2) *topological connectivity* via hierarchical graph structures that capture multi-floor layouts, and (3) *semantic extensibility* through a flexible tagging system that accommodates domain-specific information.

This work introduces a two-phase localization system that combines a physics-informed signal model with osmAG’s structural priors. The system comprises an offline phase, where an iterative optimization algorithm is employed to accurately localize all WiFi Access Points (APs). The resulting AP locations are then permanently stored as semantic tags within the osmAG map providing support for long-term robot localization. In the subsequent online phase, a mobile robot queries this augmented map to retrieve the precise AP locations and performs robust, real-time global localization. This AP-based localization offers two significant benefits over traditional fingerprint-based localization: As the experiments will show, the robot localization is significantly more accurate, especially in areas lacking fingerprints and 2) the storage size of the

<sup>1</sup>The authors are with the Key Laboratory of Intelligent Perception and Human-Machine Collaboration - ShanghaiTech University, Ministry of Education, China. {maxu2023, zhangjj2023, xiejf, soerensch}@shanghaitech.edu.cn

required data (fingerprints vs AP information) is much smaller, typically more than one order of magnitude. For comparison, we also implemented a fingerprint-based osmAG localization approach. The primary contributions of this work are:

- A WiFi AP localization framework that fuses physics-based signal modeling with osmAG’s geometric and topological priors, eliminating the need for manual AP surveying.
- An efficient real-time robot localization system exploiting the pre-calibrated AP map and osmAG’s structural insights for superior accuracy.
- Comprehensive validation across a 11,025 m<sup>2</sup> multi-floor environment, outperforming traditional fingerprinting methods in localization precision.
- The public release code of our complete localization framework and dataset, alongside a detailed specification for an osmAG-compatible representation of WiFi data.

## II. RELATED WORK

This section provides an overview of prominent global localization approaches, highlighting their methodologies, strengths, and limitations, and positioning our work within this landscape.

1) *Sensor-centric Based Localization*: Traditional localization methods rely on onboard sensors like cameras and LiDAR. Vision-based approaches [6], [7] typically extract visual features and use them for image retrieval against a geo-referenced database. However, these methods are vulnerable to lighting variations, texture deficiencies, and occlusions, which can compromise accuracy and robustness. Similarly, LiDAR-based methods [8]–[10] use geometric descriptors to match point clouds against a pre-built map. While precise, they often suffer from high computational complexity and significant storage overhead, which limits their scalability on resource-constrained platforms.

### A. WiFi-based Localization

Traditional fingerprinting approaches construct a map of Received Signal Strength Indicator (RSSI) values at known locations and then estimate a new position by matching current RSSI readings to the map. While capable of high accuracy in surveyed areas, this method is labor-intensive, sensitive to environmental changes, and suffers from poor generalization to non-fingerprinted regions.

Early work [11] utilized Gaussian Processes (GPs) to create continuous signal strength maps, offering the flexibility to model non-linear propagation and provide robust uncertainty estimates. Subsequent research enhanced this paradigm by incorporating physical path-loss models as informative priors for GPs, which improved localization accuracy, particularly in scenarios with sparse training data [2]. A key challenge in WiFi localization is the coherent fusion of data from numerous Access Points (APs). To address the overconfident estimates resulting from simplistic independence assumptions, advanced frameworks like the General Product of Experts (gPoE) were proposed to weigh the contribution of each AP based on

its information gain [3]. Other works integrated WiFi with geometric constraints or additional sensors within probabilistic frameworks like particle filters to enable autonomous navigation [1], [12].

In contrast to these approaches, our work introduces a framework that directly embeds the physical structure of the environment into the localization process. Instead of creating a dense RSSI fingerprint map for robot localization or relying on complex probabilistic models to implicitly learn environmental effects, our primary contribution is a two-phase system that first focuses on the high-fidelity localization of the APs themselves. This approach enables superior generalization to un-surveyed areas and offers a scalable solution for long-term autonomy by eliminating the need for exhaustive fingerprinting.

## III. METHOD

Our proposed large-scale indoor localization framework is architecturally divided into two primary phases: an offline phase for Access Points (APs) localization and an online phase for real-time robot localization. In the offline phase, we populate the osmAG map with the building’s geometry and a WiFi dataset comprising robot poses (w.r.t. the map frame) and synchronized WiFi RSSI measurements. An optimization algorithm then leverages this integrated data to compute the locations of all WiFi APs, explicitly modeling wall attenuation, and permanently stores these locations back into the map. Subsequently, in the online phase, the robot queries the augmented osmAG map to retrieve AP positions and wall data. By fusing these priors with live RSSI scans through a physics-informed model, the system achieves robust and accurate real-time global localization.

### A. osmAG Map Representation

The osmAG map is meticulously structured to encapsulate both the physical layout of the indoor environment and the specialized data required for WiFi-based localization. It uses XML format to store data obtained from CAD, 2D grid maps, or 3D point cloud maps [4], [13]. This representation is composed of two primary components: a geometric-topological component and a WiFi-associated component.

1) *Geometric-Topological Component*: The geometric-topological component serves as the structural backbone of the map, defining the physical architecture of the indoor space. This component is constructed using two fundamental osmAG primitives: *nodes* and *ways*, as illustrated in Figure 2.

- **Nodes**: Nodes are discrete points defined by geographical coordinates (latitude and longitude). They function as the vertices in the map’s graph structure, representing key locations such as corners of rooms, ends of corridors, or doorways.
- **Ways**: Ways are ordered sequences of nodes that define polygonal areas. By connecting nodes, ways are used to delineate structural elements like walls, corridors, and rooms.

```

<?xml version='1.0' encoding='UTF-8'?>
<osm version='0.6' generator='JOSM'>
  <!-- OSMAG Map Components Demonstration for WiFi Localization -->

  <!-- Geometric-Topological Component: Nodes defining building structure and walls -->
  <node id='-1001' latitude='31.1795000000' longitude='121.5910000000'></node>
  <node id='-1002' latitude='31.1795100000' longitude='121.5911000000'></node>
  <node id='-1003' latitude='31.1795200000' longitude='121.5912000000'></node>
  <node id='-1004' latitude='31.1795300000' longitude='121.5913000000'></node>

  <!-- Geometric-Topological Component: Ways defining building structure and walls -->
  <way id='-4001'>
    <nd ref='-1001' />
    <nd ref='-1002' />
    <nd ref='-1003' />
    <nd ref='-1004' />
    <nd ref='-1001' />
    <tag k='osmAG:areaType' v='room' />
    <tag k='name' v='E1d-F1-14' />
    <tag k='osmAG:parent' v='E1d-F1' />
    <tag k='level' v='1' />
  </way>

  <!-- WiFi Access Point Node -->
  <node id='-2001' latitude='31.1795050000' longitude='121.5910050000'>
    <tag k='osmAG:node:type' v='AP' />
    <tag k='osmAG:WiFi:BSSID' v='9c:b2:e8:92:b4:d4' />
    <tag k='osmAG:WiFi:AP:level' v='1' />
    <tag k='osmAG:WiFi:AP:name' v='1F-WiFi' />
  </node>

  <!-- WiFi Fingerprint Node with RSSI measurements and Robot Position -->
  <node id='-3001' latitude='31.17950614433' longitude='121.59099415865'>
    <tag k='osmAG:node:type' v='fingerprint' />
    <tag k='osmAG:WiFi:Fingerprint:Floor' v='1' />
    <!-- WiFi measurements from multiple APs -->
    <tag k='osmAG:WiFi:BSSID:1' v='9c:b2:e8:92:b4:d4' />
    <tag k='osmAG:WiFi:RSSI:1' v='-70.0' />
    <tag k='osmAG:WiFi:BSSID:2' v='5c:c0:a0:ac:58:b0' />
    <tag k='osmAG:WiFi:RSSI:2' v='-78.0' />
    <!-- and more -->
  </node>
</osm>

```

Fig. 2: osmAG's components description in XML format

Together, nodes and ways form a comprehensive graph that describes not only the geometry (the shape and size of rooms) but also the topology (the connectivity between different spaces, such as how corridors link various rooms).

2) *WiFi Data in osmAG*: Our osmAG format can be used to store both: fingerprint data, which is also used for AP localization, and AP data. Fingerprint data contains the time-synchronized robot position, acquired from an accurate Simultaneous Localization and Mapping (SLAM) algorithm, e.g. [14] and the corresponding WiFi Received Signal Strength Indicator (RSSI) measurements. For this we utilize of osmAG tags, which are key-value pairs associated with nodes, as illustrated in Figure 2. This figure also shows an example of an AP node.

By integrating these two components into a unified osmAG representation, we create a rich, multi-purpose map that simultaneously provides a detailed model of the physical world and the essential data for robust indoor localization.

### B. Offline Phase: AP Localization

The primary objective of the offline phase is to localize all Access Points (APs) from previously collected fingerprint data and embed their positions into the osmAG map, thereby establishing the foundational data layer required for the subsequent online robot localization.

1) *Physics-Informed Signal Propagation Model*: In this stage we utilize the ground truth positions of a few APs

(estimated by hand within the map), together with the map and some fingerprints, to estimate certain model parameters. We adopt the log-distance path loss model, a standard for describing indoor radio wave propagation. The model relates the received signal strength to the distance between a transmitter and a receiver:

$$RSSI = RSSI_0 - 10n \log_{10}(d) - \sum_k N_k W_k + X_\sigma \quad (1)$$

where  $RSSI_0$  is the reference signal strength at a distance of one meter,  $n$  is the path loss exponent,  $d$  is the 3D Euclidean distance between the AP and the robot,  $W_k$  is the attenuation factor for the  $k$ -th wall,  $N_k$  is the number of walls of  $k$  intersecting the signal path, and  $X_\sigma$  is a zero-mean Gaussian random variable representing shadowing effects. Our goal is to estimate the parameters  $RSSI_0$ ,  $n$ , and an average wall attenuation factor  $\bar{W}$ .

2) *Two-Stage Parameter Optimization*: To accurately estimate the model parameters, we employ a two-stage optimization process that leverages the geometric information from the osmAG map.

- 1) *Stage 1: LOS Parameter Estimation*. We first isolate a set of Line-of-Sight (LOS) measurements. For each AP-Robot pair from our WiFi dataset, we perform a geometric intersection test between the direct signal path and the polygons stored in the osmAG map. If no intersection occurs, the measurement is classified as LOS. Using this LOS dataset ( $\mathcal{S}_{LOS}$ ), we solve for the baseline parameters ( $RSSI_0^*, n^*$ ) via least-squares regression:

$$(RSSI_0^*, n^*) = \arg \min_{RSSI_0, n} \sum_{(i,j) \in \mathcal{S}_{LOS}} e_{ij}^2 \quad (2)$$

$$e_{ij} = RSSI_{ij} - RSSI_0 + 10n \log_{10}(d_{ij}) \quad (3)$$

where  $(i, j)$  represents the measurement pair between the  $i$ -th AP and the  $j$ -th robot position,  $RSSI_{ij}$  is the measured signal strength for this pair, and  $d_{ij}$  is the 3D Euclidean distance between the  $i$ -th AP and the  $j$ -th robot position.

- 2) *Stage 2: NLOS Wall Attenuation Estimation*. Conversely, signals whose direct path between the AP and the robot is obstructed by one or more walls are classified as Non-Line-of-Sight (NLOS) measurements. With the baseline parameters fixed, we then use NLOS measurements to estimate a single, effective wall attenuation factor  $\bar{W}$ , that will be used for all walls. This factor represents the average signal loss incurred when passing through a wall in the environment. It is computed by minimizing the residual error for all NLOS measurements:

$$\bar{W} = \arg \min_W \sum_{(i,j) \in \mathcal{S}_{NLOS}} e_{ij}^2 \quad (4)$$

$$e_{ij} = RSSI_{ij} - RSSI_0^* + 10n^* \log_{10}(d_{ij}) - N_{ij} \bar{W} \quad (5)$$

where  $N_{ij}$  is the number of walls intersecting the path between measurement  $i$  and  $j$ .

3) *Iterative AP Position Estimation*: With the environmental parameters ( $\text{RSSI}_0^*, n^*, \bar{W}$ ) established, we proceed to estimate the unknown position of each AP. This is formulated as an iterative optimization problem.

- 1) *Initialization*: For a target AP, we first convert all its associated RSSI measurements from the WiFi dataset into initial distance estimates  $\hat{d}_i$  between AP and robot, using the LOS model:

$$\hat{d}_i = 10^{(\text{RSSI}_0^* - \text{RSSI}_i) / (10n^*)}. \quad (6)$$

We then compute an initial 3D position estimate  $\mathbf{p}_{\text{AP}}^{(0)}$  by solving a least-squares minimization problem :

$$\mathbf{p}_{\text{AP}}^{(0)} = \arg \min_{\mathbf{p}} \sum_{i=1}^N \left( \|\mathbf{p} - \mathbf{p}_i\| - \hat{d}_i \right)^2 \quad (7)$$

where  $\mathbf{p}_i$  are the known coordinates of the  $i$ -th robot position. This initial estimate, as shown in the left panel of Figure 3, typically exhibits significant deviation from the ground truth location due to the lack of environmental geometry consideration.

- 2) *Iterative Refinement*: We refine this initial estimate over a fixed number of iterations. At each iteration  $t$ :

- a) We perform wall intersection tests between the current AP position estimate  $\mathbf{p}_{\text{AP}}^{(t-1)}$  and all robot positions  $\mathbf{p}_i$ .
- b) For each measurement classified as NLOS, we compute a compensated distance estimate  $\hat{d}_i^{(t)}$  by accounting for wall attenuation:

$$\hat{d}_i^{(t)} = 10^{(\text{RSSI}_0^* - (\text{RSSI}_i + N_i \bar{W})) / (10n^*)} \quad (8)$$

where  $N_i$  is the number of walls detected on the path. For LOS measurements, the distance estimate remains uncompensated.

- c) We solve the least-squares problem again with these refined distance estimates to obtain the updated AP position  $\mathbf{p}_{\text{AP}}^{(t)}$ .

The right panel of Figure 3 illustrates the final, refined position after applying our iterative optimization framework, showing how the algorithm converges to a significantly more accurate estimate that moves much closer to the ground truth. This iterative process allows the APs' position estimate to converge to a solution that is consistent with both the signal strength measurements and the physical geometry of the environment.

### C. Online Phase: Real-Time Robot Localization

In the online phase, the robot uses the augmented osmAG map from the offline phase containing the now-known AP locations and environmental parameters to determine its own position in real time.

- 1) *Real-Time Data Acquisition*: The robot continuously scans for WiFi signals, collecting RSSI measurements over

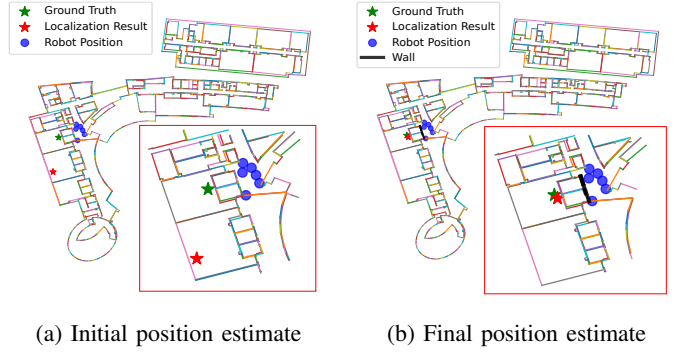


Fig. 3: Iterative AP localization for a single Access Point. (a) Initial estimate using a log-distance model, showing significant deviation from the ground truth (green star). (b) Final estimate after iterative optimization with wall attenuation, converging closer to the ground truth after 10 times iterations. Blue points represent robot positions, and the red box highlights a zoomed-in view of the final estimate.

a brief temporal window (e.g., 3-5 seconds) and averaging them to ensure signal stability for the subsequent localization process.

- 2) *Iterative Position Estimation*: The robot's position is estimated using an iterative optimization framework analogous to the one used for AP localization.

- 1) *Initialization*: An initial 3D position estimate  $\mathbf{p}_{\text{robot}}^{(0)}$  is computed via trilateration using the detected APs and their known locations from the osmAG map.
- 2) *Iterative Refinement*: The robot's position is refined iteratively. At each iteration  $t$ , the system performs wall intersection checks between the current robot position estimate  $\mathbf{p}_{\text{robot}}^{(t-1)}$  and all visible APs. It then calculates compensated distance estimates and solves a least-squares problem to find the updated position  $\mathbf{p}_{\text{robot}}^{(t)}$ :

$$\mathbf{p}_{\text{robot}}^{(t)} = \arg \min_{\mathbf{p}} \sum_{k=1}^K \left( \|\mathbf{p} - \mathbf{p}_k^{\text{AP}}\| - \hat{d}_k^{(t)} \right)^2 \quad (9)$$

where  $\mathbf{p}_k^{\text{AP}}$  is the known position of the  $k$ -th visible AP and  $\hat{d}_k^{(t)}$  is its corresponding compensated distance estimate. The process terminates when the change in position between iterations falls below a predefined threshold ( $\|\mathbf{p}_{\text{robot}}^{(t)} - \mathbf{p}_{\text{robot}}^{(t-1)}\| < \epsilon$ ) or a maximum number of iterations is reached.

## IV. EXPERIMENTS

In this section, we conducted extensive experiments to validate both the access points (APs) localization accuracy and the robot localization performance.

### A. Experimental Setup

Our experiments were conducted in a multi-floor indoor environment at ShanghaiTech University, covering 11,025 m<sup>2</sup> across two floors and two buildings, as illustrated in Figure 4. The environment, comprising classrooms, labs, and offices



with various wall types (concrete, drywall, glass), provided realistic signal propagation conditions. We used an Agilent Hunter SE mobile platform equipped with an EDUP EP-AC1681 WiFi receiver and a Hesai 64-channel LiDAR for data acquisition. LIO-SAM [14] was used to obtain ground truth robot positions, while 48 AP ground truths were manually surveyed.

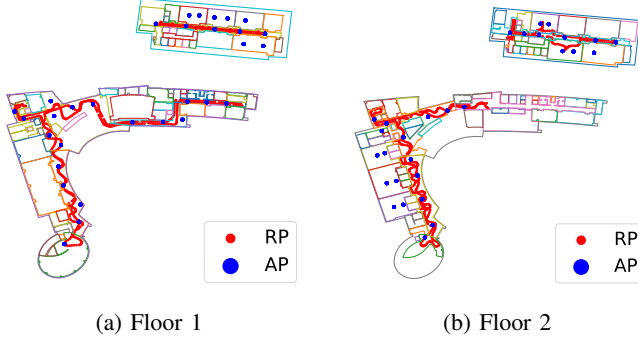


Fig. 4: osmAG layout of the SIST and SEM buildings at ShanghaiTech University, spanning  $11,025 \text{ m}^2$  across two floors. (a) Floor 1 and (b) Floor 2, showing robot positions (RP) and ground truth Access Points positions used for localization experiments, rendered using matplotlib [15].

### B. Parameter Learning

To instantiate our physics-informed signal propagation model, we first conducted a dedicated parameter learning phase. We selected the first floor of the SIST building as our training area, which is representative of the complex environment where the framework is to be deployed. The optimization yielded the following values:

- Reference Signal Strength ( $\text{RSSI}_0^*$ ): -28.79
- Path Loss Exponent ( $n^*$ ): 2.5
- Wall Attenuation Factor ( $\bar{W}$ ): -10.77

These learned parameters were then fixed and applied consistently throughout all subsequent experiments for both AP localization and robot localization.

### C. Access Point Localization Results

We use the WiFi data collected at robot positions in Figure 4 to locate the APs and compare it with the ground truth. To evaluate our AP localization algorithm, we first established a baseline using conventional trilateration, which represents the initial, geometry-unaware state of our iterative process. This approach yielded a mean localization error of 5.86 m with a standard deviation of 7.82 m across the 48 ground-truthed APs. As depicted in Figure 5, the initial estimates produced a wide error distribution, underscoring the inherent limitations of ignoring physical obstructions.

Applying our iterative optimization algorithm, which leverages geometric data from the osmAG map to compensate for wall attenuation, yielded a significant improvement. Our physics-informed framework reduced the mean localization

error to 3.79 m with a standard deviation of 2.52 m, a 35.3% improvement over the baseline. As illustrated in Figure 5, the error distribution for the optimized results is visibly shifted towards zero and is significantly more compact, indicating a higher degree of both accuracy and precision. This significant enhancement in performance is directly attributable to our framework’s ability to integrate the physical reality of the environment. The convergence to a more accurate and consistent set of AP positions validates that a physics-informed model is essential for robust WiFi-based localization in large-scale indoor environment.

Comparative Analysis of AP Localization Error Distributions

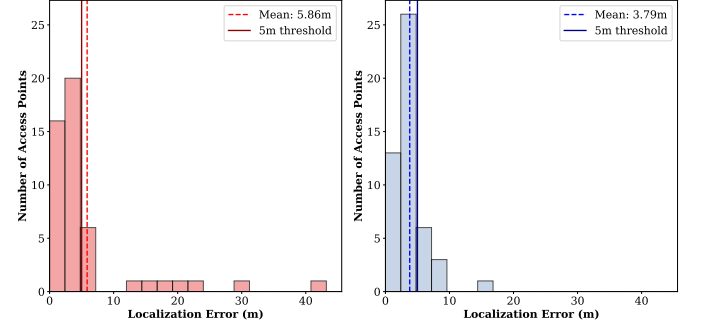


Fig. 5: Error distribution for AP localization. The initial geometry-unaware trilateration (left diagram; mean error: 5.86 m) is compared to our iterative optimization (right diagram; mean error: 3.79 m), showing a tighter distribution and 35.3% error reduction.

Storing AP data in osmAG is much more space-efficient than fingerprints: The osmAG of this experiment without any WiFi data is 708kb, the fingerprint data is additionally 11,068kb for 1491 prints (7.4kb per print), while the AP data is just 44kb for 48 APs (<1kb per AP), 215 times smaller than the fingerprints.

### D. Robot Localization Results

To comprehensively evaluate the real-time robot localization performance of our system, we designed two distinct experimental scenarios within the multi-floor test environment. For comparison, we benchmarked our physics-informed method against a traditional K-Nearest Neighbors (KNN) fingerprinting algorithm, a widely used baseline in WiFi localization.

1) *Localization within Fingerprinted Areas*: The first scenario assesses localization accuracy at 66 test points within fingerprinted areas (near red robot positions area in Figure 4), as illustrated in Figure 6. The objective of this test was to evaluate the system’s performance under ideal conditions where ample reference data is available. The results, summarized in Table I, indicates that our method achieves a slightly lower mean localization error, demonstrating its effectiveness compared to the fingerprinting algorithm.

2) *Generalization to Non-Fingerprinted Areas*: The second, more challenging scenario was designed to assess the system’s generalization capability. The robot was tasked with localizing

TABLE I: Quantitative Comparison of Robot Localization Performance Across Different Scenarios

Scenario	Method	Mean Error (m)	Std. Dev. (m)	RMSE (m)	95% Percentile (m)
Fingerprinted Areas	Fingerprinting	3.42	2.50	4.24	7.85
	<b>Ours</b>	<b>3.12</b>	<b>1.35</b>	<b>3.34</b>	<b>4.65</b>
Non-Fingerprinted Areas	Fingerprinting	20.21	9.48	22.32	36.18
	<b>Ours</b>	<b>3.83</b>	<b>0.78</b>	<b>3.91</b>	<b>4.72</b>

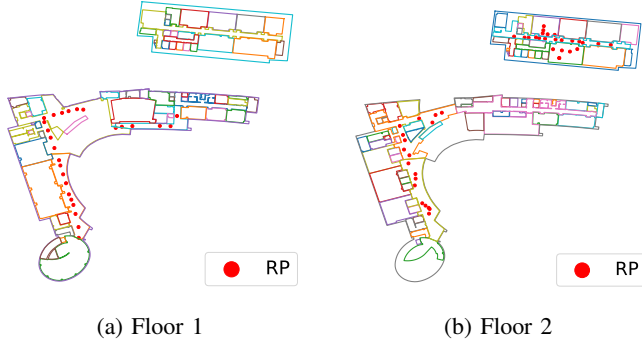


Fig. 6: Distribution of 66 test points for robot localization in fingerprinted areas of the SIST and SEM buildings.

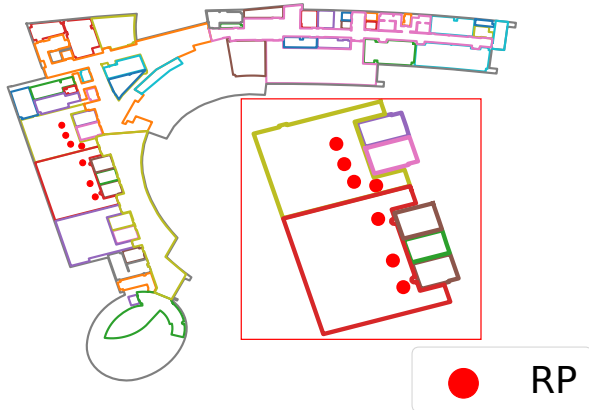


Fig. 7: Robot localization test point in a non-fingerprinted region of the environment (SEM Floor 2). The red box in the lower right corner is a partial enlargement.

itself at multiple positions that were excluded from the fingerprinted areas (faraway red robot positions area in Figure 4), as shown in Figure 7. This experiment simulates a practical use-case where a robot must operate in areas of a building for which no specific WiFi data has been pre-collected. In this scenario, the performance of the traditional KNN fingerprinting method degraded significantly, as it struggled to extrapolate beyond its training data. In contrast, as detailed in Table I, our method of robot localization via localized AP positions produced a significantly lower localization error, demonstrating its robustness and practical applicability for large-scale deployment where exhaustive fingerprinting is infeasible.

## V. CONCLUSIONS

In this paper, we introduced a novel physics-informed global WiFi localization method that leverages structural priors from osmAG to enable robust and efficient robot localization in large-scale environments. By integrating a physics-based WiFi signal propagation model with building structural information, our approach surpasses conventional fingerprinting methods, particularly in areas with sparse WiFi data. Our framework provides a reliable, coarse initial pose estimate for a mobile robot, solving the kidnapped robot problem. Our experiments show that our AP localization works well, that storing AP information in osmAG is much more space efficient than fingerprint data and that the robot localization of our approach is superior to fingerprint approaches, especially in areas for which no fingerprint data is available. This WiFi localization can act as the prior for our approach to robust lifelong indoor LiDAR localization with osmAG [16].

We plan to further develop the WiFi localization methods, for example by learning the wall parameters and AP positions without needing some initial ground truth AP positions, employing more advanced optimization methods. We will also integrate our methods into a complete osmAG navigation stack.

## ACKNOWLEDGMENT

The experiments of this work were supported by the core facility Platform of Computer Science and Communication, SIST, ShanghaiTech University.

## REFERENCES

- [1] J. Biswas and M. Veloso, "Wifi localization and navigation for autonomous indoor mobile robots," in *2010 IEEE International Conference on Robotics and Automation*, 2010, pp. 4379–4384.
- [2] R. Miyagusuku, A. Yamashita, and H. Asama, "Improving gaussian processes based mapping of wireless signals using path loss models," in *2016 IEEE/RSJ International Conference on Intelligent Robots and Systems (IROS)*, 2016, pp. 4610–4615.
- [3] —, "Data information fusion from multiple access points for wifi-based self-localization," *IEEE Robotics and Automation Letters*, vol. 4, no. 2, pp. 269–276, 2019.
- [4] D. Feng, C. Li, Y. Zhang, C. Yu, and S. Schwertfeger, "osmag: Hierarchical semantic topometric area graph maps in the osm format for mobile robotics," in *2023 IEEE International Conference on Robotics and Biomimetics (ROBIO)*, 2023, pp. 1–7.
- [5] OpenStreetMap Wiki contributors, "Josm," <https://wiki.openstreetmap.org/wiki/JOSM>, 2024, [Online; accessed 17-June-2025].
- [6] S. Matsuzaki, T. Sugino, K. Tanaka, Z. Sha, S. Nakaoka, S. Yoshizawa, and K. Shintani, "Clip-loc: Multi-modal landmark association for global localization in object-based maps," in *2024 IEEE International Conference on Robotics and Automation (ICRA)*, 2024, pp. 13 673–13 679.
- [7] M. Altillawi, Z. Pataki, S. Li, and Z. Liu, "Global localization: Utilizing relative spatio-temporal geometric constraints from adjacent and distant cameras," in *2023 IEEE/RSJ International Conference on Intelligent Robots and Systems (IROS)*, 2023, pp. 3358–3365.

- [8] M. Shaheer, J. A. Millan-Romera, H. Bavle, J. L. Sanchez-Lopez, J. Civera, and H. Voos, "Graph-based global robot localization informing situational graphs with architectural graphs," in *2023 IEEE/RSJ International Conference on Intelligent Robots and Systems (IROS)*, 2023, pp. 9155–9162.
- [9] J. Lv, C. Meng, Y. Wang, J. Sun, R. Xiong, and S. Pu, "So-pfh: Semantic object-based point feature histogram for global localization in parking lot," in *2022 IEEE/RSJ International Conference on Intelligent Robots and Systems (IROS)*, 2022, pp. 4431–4438.
- [10] K. Aoki, K. Koide, S. Oishi, M. Yokozuka, A. Banno, and J. Meguro, "3d-bbs: Global localization for 3d point cloud scan matching using branch-and-bound algorithm," in *2024 IEEE International Conference on Robotics and Automation (ICRA)*, 2024, pp. 1796–1802.
- [11] B. Ferris, D. Haehnel, and D. Fox, "Gaussian Processes for Signal Strength-Based Location Estimation," in *Robotics: Science and Systems II*, Aug. 2006.
- [12] S. Ito, F. Endres, M. Kuderer, G. Diego Tipaldi, C. Stachniss, and W. Burgard, "W-rgb-d: Floor-plan-based indoor global localization using a depth camera and wifi," in *2014 IEEE International Conference on Robotics and Automation (ICRA)*, 2014, pp. 417–422.
- [13] J. Zhang, S. Wu, X. Ma, and S. Schwertfeger, "Generation of indoor open street maps for robot navigation from cad files," 2025. [Online]. Available: <https://arxiv.org/abs/2507.00552>
- [14] T. Shan, B. Englot, D. Meyers, W. Wang, C. Ratti, and D. Rus, "Lio-sam: Tightly-coupled lidar inertial odometry via smoothing and mapping," in *2020 IEEE/RSJ International Conference on Intelligent Robots and Systems (IROS)*, 2020, pp. 5135–5142.
- [15] J. D. Hunter, "Matplotlib: A 2d graphics environment," *Computing in Science & Engineering*, vol. 9, no. 3, pp. 90–95, 2007.
- [16] F. Xie and S. Schwertfeger, "Robust lifelong indoor LiDAR localization using the area graph," *IEEE Robotics and Automation Letters (RA-L)*, vol. 8, no. 12, pp. 8163–8170, 2023.